A Hybrid Pedestrian Detection System based on Visible Images and LIDAR Data

Mohamed El Ansari[1], Redouan Lahmyed[1] and Alain Tremeau[2]
[1]*LabSIV, Department of Computer Science, Faculty of Science, University of Ibn Zohr, Agadir, Morocco*
[2]*Hubert Curien Laboratory, University Jean Monnet, Saint-Etienne, France*

Keywords: Pedestrian Detection, LIDAR Sensor, Visible Camera Sensor, Support Vector Machines (SVMs), Adaboost, Histogram of Oriented Gradients (HOG), Local Self-similarity (LSS).

Abstract: This paper presents a hybrid pedestrian detection system on the basis of 3D LIDAR data and visible images of the same scene. The proposed method consists of two main stages. In the first stage, the 3D LIDAR data are classified to obtain a set of clusters, which will be mapped into the visible image to get regions of interests (ROIs). The second stage classifies the ROIs (pedestrian/non pedestrian) using SVM as classifier and color based histogram of oriented gradients (HOG) together with the local self-similarity (LSS) as features. The proposed method has been tested on LIPD dataset and the results demonstrate its effectiveness.

1 INTRODUCTION

Advanced Driver Assistance Systems (ADAS) is an active research area that has attracted a lot of interest in the recent years, due to the fact that it plays an important role at enhancing vehicle systems for safety and better driving to avoid collisions and accidents. There are various sensors upon which ADAS technology is based, such as the visible cameras (Lim and Kim, 2013; Zhang et al., 2016), thermal cameras (Yang et al., 2016; Elguebaly and Bouguila, 2013), LIDAR sensors (Lahmyed and El Ansari, 2016; Premebida and Nunes, 2006) and so on. The diverse kinds of data acquired from those sensors could be exploited in many ADAS fields such as pedestrian detection (Zhu and Peng, 2017), traffic sign detection and recognition (Ellahyani and El Ansari, 2017; Ellahyani et al., 2016), vehicle environment perception (Ilyas El Jaafari et al., 2017; El Jaafari et al., 2016; Mazoul et al., 2014; El Ansari et al., 2010) and so on. One of the major challenges that ADAS face is the comprehension of the environment and directing the vehicles in real outdoor scenes (Prieto and Allen, 2009). For that, the requirement of determining and identifying the presence of pedestrians in the scene is considered as a crucial task.

The purpose of a pedestrian detection system is to find out the presence of both moving and stationary humans in a particular area of interest around the moving vehicle in order alert the driver. However, there are many factors that make the pedestrian detection problem difficult such as:

- The appearance of pedestrians shows very wide variability: High variety of poses, wear different clothes, carry diverse objects and have a considerable range of sizes.
- Complex backgrounds: the pedestrians must be well detected in outdoor urban scenarios despite the wide range of illumination and weather conditions that affect the quality of the sensed information.
- Occlusions and different scales between pedestrians as well as the appearance of the pedestrians at different viewing angles.

In this paper, we present a new pedestrian detection approach that includes both LIDAR and vision sensors. The proposed approach is an extension of that early presented in (Lahmyed and El Ansari, 2016) by the same authors. It takes as input a 3D LIDAR data and its corresponding visible image. The proposed approach is composed of two major stages. The first stage clusters the 3D LIDAR data into connected components using the DBSCAN (Ester et al., 1996) technique. The obtained clusters are projected on the corresponding visible image to generate ROIs. The second stage identifies the pedestrians from the extracted ROIs using the Color-based HOG feature combined with LSS feature that they are provided to the SVM classifier.

Ansari, M., Lahmyed, R. and Tremeau, A.
A Hybrid Pedestrian Detection System based on Visible Images and LIDAR Data.
DOI: 10.5220/0006620803250334
In *Proceedings of the 13th International Joint Conference on Computer Vision, Imaging and Computer Graphics Theory and Applications (VISIGRAPP 2018) - Volume 5: VISAPP*, pages 325-334
ISBN: 978-989-758-290-5

The rest of the paper is organized as follows. Section 2 presents an overview of recent works on pedestrian detection. Section 3 details the new proposed pedestrian detection method. Experimental results are presented in Section 4. Section 5 concludes the paper.

2 RELATED WORK

Different pedestrian methods have been suggested in the literature. Comparing between those approaches is a challenging task since they use different data recorded from various sensors such as visible camera (Lim and Kim, 2013; Zhang et al., 2016), infrared camera (Yang et al., 2016; Elguebaly and Bouguila, 2013), LIDAR sensor (Lahmyed and El Ansari, 2016; Premebida and Nunes, 2006), and so on.

Compared to other sensors, visible cameras (Lim and Kim, 2013) are more suited for pedestrian detection approaches due to its low cost. Those works could be classified into two main categories. The first one is based on the idea of presenting the human body as a set of parts (Cho et al., 2012; Wu and Nevatia, 2005; Mikolajczyk et al., 2004) called part-based detection. The second one tries to detect the whole body without modelling it as collection of parts, named Holistic detection (Dalal and Triggs, 2005; Papageorgiou and Poggio, 1999). Both categories adopted for pedestrian detection share the same direction in the aim of creating robust features (Tang and Goto, 2010; Mu et al., 2008; Dalal and Triggs, 2005; Lowe, 2004) using ad-hoc features or learning features (Schölkopf and Smola, 2002; Viola and Jones, 2001; Friedman et al., 2000).

In the first direction, different features have been exploited including Haar (Viola et al., 2003), Local Binary Pattern (LBP) (Ojala et al., 1996), Local Self-Similarity (LSS) (Shechtman and Irani, 2007), Histogram of Oriented Gradient (HOG) (Dalal and Triggs, 2005) and so on. Histogram of oriented gradients (HOG) features has been widely utilized in many studies and being the basis of many current detectors due to its robustness for the variation of human shape, height as well as clothes color. Local Binary Patterns (LBP) (Ojala et al., 1996) was first proposed for texture classification. LBP-based features for human detection have been suggested in (Tang and Goto, 2010; Mu et al., 2008).

In the second direction, different learning algorithms have been introduced. Boosting (Friedman et al., 2000) and SVM methods (Schölkopf and Smola, 2002) are two famous training methods in the field. Boosting methods (Viola and Jones, 2001) are generally utilized in cascade detector. They provide a satisfying performance by constructing a strong classifier using a set of weak ones. In SVM methods, the simplicity of the training phase can grant the possibility of accelerating the SVM based detection using a Multi-core CPU and a GPU in the feature extraction part. Zhang et al. (Zhang et al., 2010) introduced HOG feature and linear SVM-based human detection system. Zhu et al. (Zhu et al., 2006) presented a system that integrates the cascade of rejectors concept with the HOG feature and the Adaboost. Mikolajczyk et al. (Mikolajczyk et al., 2004) suggested a system for human detection using probabilistic assembly of robust part detectors. They used the Adaboost classifier to combine the weak classifiers to produce a fast and strong one. The Adaboost classifier has been used to construct a cascade of simple features to create a system for detecting faces (Viola and Jones, 2004) and to build a pedestrian detection system (Viola et al., 2003) using appearance and motion information.

In order to alleviate difficulties related to visible cameras, some relevant works on object classification in urban scenarios suggest to use data acquired from the laser detection and ranging (LIDAR) (Gidel et al., 2008; Premebida and Nunes, 2006; Streller and Dietmayer, 2004; Dietmayer et al., 2001). Premebida and Nunes (Premebida and Nunes, 2006) proposed the utilization of a GMM classification system over a set of geometric features for pedestrian detection in outdoor environments. In (Xavier et al., 2005), the authors proposed a new type of features named inscribed angle variance (IAV), which performs a leg-segment feature correspondence to detect persons in indoor environments. In (Arras et al., 2007), Arras et al. used a set of statistical primitives such as number of points, mean average deviation from median, standard deviation and eleven more, supplying them as an input to Adaboost classifier.

Some works propose combining the information acquired by both the LIDAR and the visible camera to increase the detection performance (Premebida et al., 2009b; Spinello and Siegwart, 2008; Douillard et al., 2007). In (Spinello and Siegwart, 2008), a pedestrian detection method based on combining visible and LIDAR sensors information has been presented. A Bayesian fusion is called together with linear SVM to perform the detection task. Douillard et al. (Douillard et al., 2007) introduced a system to detect and recognize the objects using vision and laser information in outdoor environments by taking advantage of the spatial and temporal dependencies.

3 PROPOSED METHOD

The proposed algorithm takes as input a set a 3D LIDAR data and one visible image of the same scene. The 3D LIDAR data is used to extract ROIs while the visible image image is used to classify each of the extracted ROIs as pedestrian or non pedestrian. The proposed method is achieved in two main steps: (1) ROIs extraction based on the LIDAR data and ROIs classification based on the information issued from the visible image. Here, we detail each of the two steps.

3.1 ROIs Extraction

The 3D points acquired by the LIDAR sensor are clustered into a set of groups using DBSCAN clustering technique, which was introduced in (Ester et al., 1996). It is a density-based clustering algorithm. Starting from a set of points in some space, the DBSCAN algorithm groups together points with many nearby neighbours. It considers as outliers points whose nearest neighbours are too far away. The algorithm requires two important input parameters such as *MinPts* the minimum number of points required to form a dense region and *EPS* the maximum radius of the neighbourhood from a point p. More details on how the DBSCAN works can be found in (Ester et al., 1996).

The DBSCAN clustering stage provides a set of clusters. As shown in Figure 1, the obtained clusters are represented with white spots. The points in the border of the clusters are projected to their equivalent pixels in the image captured by camera. Each cluster will generate a ROI in the corresponding image. To transform the points in the border of a cluster to their equivalent pixels, the calibration method proposed in (Zhang and Pless, 2004) is used by considering the camera extrinsic and intrinsic parameters and the LIDAR-camera coordinate transformation matrix.

3.2 ROIs Classification

Once the candidate ROIs are generated, they are given to the classification module to classify them as pedestrians or non-pedestrians. In the classification module, the computed features describing the pedestrian are fed to a classifier in order to identify. The features and classifier we adopt for the proposed method are selected based on the experiments we perform on the LIPD dataset (Premebida and Nunes, 2016).

3.2.1 Adaboost

Adaboost "Adaptive Boosting" was introduced first by Yoav Freud and Robert Schapire (Freund et al., 1999) in an attempt to select a small number of critical visual features from a very large set of potential ones. It provides an effective learning algorithm and strong bounds on generalization performance. Adaboost focuses new experts on examples that others get wrong and it trains experts sequentially. The errors of early experts indicate the hard examples. It focuses later classifiers on getting these examples right. In the end, the whole set is combined into one class, i.e., many weak learners are converted into one complex classifier.

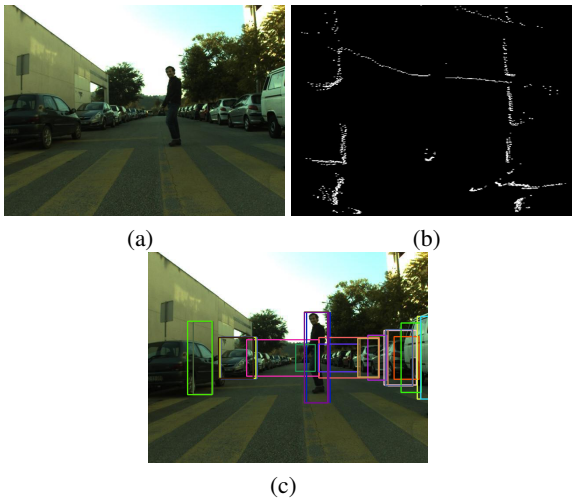

(a) (b)

(c)

Figure 1: (a) A visible image. (b) Its corresponding clusters of range points using DBSCAN algorithm as seen from above (upside view). (c) The mapped clusters on the visible image.

3.2.2 Support Vector Machine (SVM)

SVM is a classifier derived from statistical learning theory by Vapnik (Vapnik and Vapnik, 1998), and some extensive introductions were presented later in (Burges, 1998) and (Christiannini and Shawe-Taylor, 2000). SVM aims to separate the positive samples (pedestrian) from negative ones (non-pedestrian). It was introduced in the purpose of solving binary classifications. The training data are labelled $\{x_i, y_i\}$, where $i = 1, ..., nb$, $y_i \in \{-1, 1\}$, $x_i \in \{R^d\}$.
In our case, the x_i are the vectors computed by applying our proposed descriptor on the samples described above. The values y_i are "1" for one class (pedestrian) and "-1" for the others, d is the dimension of the vector, and nb is the number of training vectors.
If a hyperplane $\{w, b\}$ separates the two classes, the points that lie on it satisfy $x.w^T + b = 0$ where w is normal to the hyperplane, $|b|/\|w\|$ is the perpendicular distance from the hyperplane to the origin, and $\|w\|$ is the Euclidean norm of w.
In the separable case, the following constraints are

verified:

$$y_i(x_i.w^T + b) - 1 \geq 0 \qquad \forall i = 1..nb. \qquad (1)$$

The points for which the equality in (1) holds are located on the two hyperplanes: $H1 : x_i.w^T + b = 1$ and $H2 : x_i.w^T + b = -1$. Consequently, the margin between the two data sets is equals $2/\|w\|$. The margin can be maximized by minimizing between both sets $\|w\|^2/2$ under the constraints (1).

If we set positive Lagrange multipliers (α_i,where $i = 1,...,nb$) one for every of the inequality constraints, the objectif now will be to reduce or minimize Lp given by:

$$Lp = \frac{1}{2}\|w\|^2 - \sum_{i=1}^{nb} \alpha_i y_i (x_i.w^T + b) + \sum_{i=1}^{nb} \alpha_i. \qquad (2)$$

Once the optimization is done, we can easily decide on which part of the hyperplane a given test vector x belongs.
The decision function is given by:

$$f(x) = sgn(x.w^T + b). \qquad (3)$$

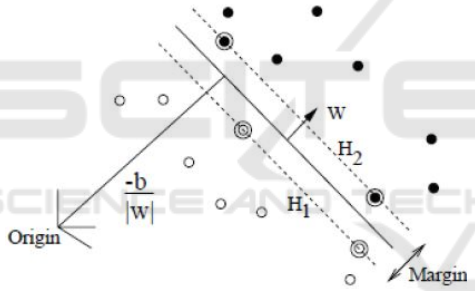

Figure 2: The margin between the two datasets.

In this paper, we have utilized not only a linear function but we used a Gaussian kernel as well, as follows:

$$K(x_i, x_j) = e^{-\frac{\|x_i - x_j\|^2}{2\sigma^2}} \qquad (4)$$

and the decision function for a new input vector is :

$$f(x) = sgn(\sum_{i=1}^{N_s} \alpha_i y_i K(s_i, x) + b). \qquad (5)$$

3.2.3 Feature Extraction

Here we describe the features (HOG, LBP and LSS) utilized in the second step of the proposed approach. To decide which of those features could be used in the pedestrian detection problem, a comparison is made. The HOG (Dalal and Triggs, 2005) is one of the feature descriptors used in computer vision and image processing aiming to detect an object in the image. The fundamental idea behind the HOG descriptor is that the local object appearance and shape within an image can be depicted pretty well by the distribution of intensity gradients or edge directions, even without accurate knowledge of the corresponding gradient or edge positions. A preprocessing step is performed before the HOG computation by converting the image into grayscale for the purpose of simplifying the computations. However there are many disadvantages of this conversion. This process removes all color information, leaving only the luminance of each pixel, which means that the specific information captured in the three color channels has been permanently lost, affecting the quality of the HOG features. We believe that extracting HOG from color images could enhance the quality of the classification. The classical manner of using the color information in HOG descriptor is based on concatenating the obtained three HOG vectors derived separately from the three color channels to create RGB-HOG descriptor. However, the computed RGB-HOG is three times longer than the grayscale HOG descriptor. Therefore, the required computational time is proportionally increased.

In this paper, we introduce a new approach in which we compute the HOG features using the color components in such a way that the final descriptor has the same size as the HOG descriptor computed from grayscale images. As a result, we preserve the color information without increasing the computational time. The new HOG descriptor, named HOG-Color, will be computed by following the same steps as the classical one (HOG derived from grayscale image) excluding the gradient magnitude and orientation step, where we use those corresponding to the color component that maximizes the gradient magnitude.

Contrary to the grayscale-base HOG, the new HOG descriptor is generated for the gradient values computed based on the color information of the image while preserving the same size as the classical HOG.

The second feature adopted in our experiments is the LBP, which was introduced in (Ojala et al., 1996). It describes the surrounding of a pixel by generating a bit-code from the binary derivatives of a pixel. The LBP operator labels the pixels of an image by thresholding the 3×3 neighborhood of each pixel with the center value and converts the result into a binary numbers defined by equation (6).

$$LBP(x_i) = \sum_{i=1}^{T} s(I_i - I_c)2^i \qquad (6)$$

such that

$$s(I_i - I_c) = \begin{cases} 1 & I_i - I_c \geq 0 \\ 0 & I_i - I_c \leq 0 \end{cases}. \qquad (7)$$

where I_c and I_i are the grey value of image and T is the total number of involved neighbours.

The performance of the HOG decreases when the background is cluttered with noisy edge points (Ojala et al., 1996). To avoid that, the concatenation between the HOG and LBP features is made in order to create new features named HOG+LBP that allow reducing the effect of the noise on the classification results. Given that the result obtained by HOG-Color is better than the classic grayscale HOG and RGB-HOG, the concatenation HOG-Color with LBP called HOG-Color+LBP is used instead of HOG+LBP and RGB-HOG+LBP, respectively.

The third feature involved in this paper is LSS (Shechtman and Irani, 2007). This feature has the ability of capturing the internal geometric layouts of local self-similarities within image, while accounting for small local affine deformations as well as capturing self-similarity of edges, color, repetitive patterns and complex textures in a single unified manner. In LSS features, we divide the chosen image into several patches which, efficiently compared with a cell located at center of the image. Then, we normalize the obtained distance and we project it into the space intervals divided by radial intervals and the number of angle intervals. We take the extreme value in an interval space as the value of the feature.

LSS features was concatenated with the HOG-Color features to build a descriptor, called HOG-Color+LSS. This descriptor is used by a classifier to classify pedestrians.

In this paper, a comparison between many features is made to determine which ones gives the best results. First, we used a simple HOG on grayscale image. Then, we computed the HOG from the colored image named HOG-Color. Furthermore, the new HOG-Color is combined with LBP to build an augmented feature vector. Another combination of HOG-Color with LSS is made to create one more feature vector.

4 EXPERIMENTAL RESULTS

This section presents the results obtained by the proposed approach. Different experiments have been performed on the LIPD dataset to evaluate the performances of the classifiers as well as the features introduced in the preceding section. All the experiments have been performed using the processor Intel (R) core (TM) i5-2430M CPU 2.4 GHz.

4.1 Dataset

The Laser and Image Pedestrian Detection Dataset (LIPD) (Premebida and Nunes, 2016) has been used to test the performance of the proposed system. The LIPD Dataset was collected in outdoor conditions (the Coimbra Univeristy/ISR Campus zone). It was recorded using Yamaha-ISR electric vehicle (IS-RobotCar), equipped with a multilayer automotive laserscanner Alasca-XT from Ibeo, a TopCon Hyper-Pro GPS device in RTK mode, one IMU Mti from Xsens and a monocular Guppy camera. The LIPD dataset contains 4823 frames (one frame is composed of one visible image and its corresponding LIDAR data). The images format is 24-bit color jpg and their size is 640 x 480 pixels.

4.2 Parameters Setting

The parameters involved in the various modules of the proposed system were selected empirically using images from LIPD dataset. In the first stage, two parameters of DBSCAN clustering algorithm were utilized: EPS and the minimum number of points needed to compose a dense region ($MinPts$). Figure 3 (a) clarifies the number of true positives (TPs) and Figure 3 (b) shows the computing time, while varying these two parameters over 900 images chosen from the LIPD dataset. Notice that a correct detected person is counted true positive if its corresponding bounding box overlaps with at least 70 % of the area covered by the person present in the image. We observe that the number of true positives is not quite sensitive to EPS parameter. However, the computing time increments with these two parameters. $EPS = 5$, and $MinPts = 400$ are chosen since they guarantee high accuracy (more than 890 true positives) while the computational time is at its lowest value (less than 40 ms).

To get the optimal parameters of the classifiers utilized in the system, cross-validation experiments have been achieved on a training dataset. The images of the dataset are divided into a training and validation subsets. By training and testing the classifiers on the two subsets using various parameters settings, the parameters that enable to get the high classification accuracy have been selected. The classifiers have been retrained again using the chosen parameters on the LIPD training dataset. In this work, we use SVM with radial basis function (RBF) kernel with C=2 and G=0.03. The classification accuracy varies while changing the value of these two parameters and become higher as these parameters reach the values 2 and 0.03, respectively, for all the features used.

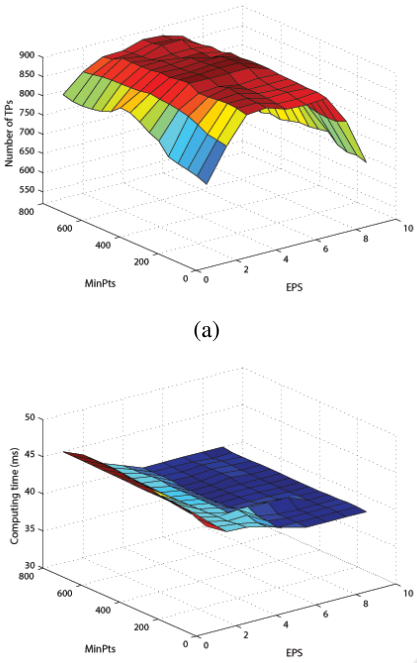

(a)

(b)

Figure 3: Number of TPs and the computing time while changing *EPS* and *MinPts*.

4.3 Results

An example of detection results is provided in Figure 4. The algorithm takes an image (Figure 4 (a)) and its corresponding 3D LIDAR data as input. The clustering results are depicted in Figure 4 (b). The ROIs obtained based on the mapping of the clusters (Figure 4 (b)) on the image (Figure 4 (a)) are showed in Figure 4 (c). A number of ROIs were detected even if they did not represent pedestrians meanwhile they represented other objects in the road scene. In the aim of rejecting these ROIs, we refer to the classification step. The detected ROIs are classified into pedestrians or non-pedestrians using the HOG-Color and LSS features together with SVM classifier. The classification results are illustrated in Figure 4 (d). Only three ROIs have been classified as pedestrians, while the other ROIs have been discarded. The green bounding boxes correspond to the detected pedestrians. The running time of each one of the previous steps is represented in Table 1. The required time for the whole detection method is 39.82 + 49.11= 88.93 ms.

Table 1: The computing time of each step of the proposed approach in ms/f.

	ROIs extraction	ROIs classification
Consuming time (ms)	39.82	49.11

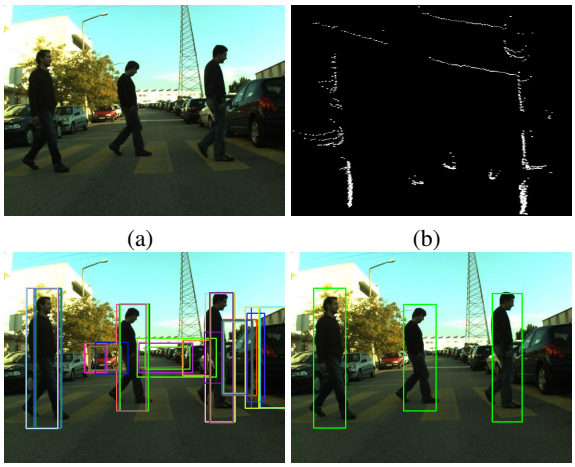

(a) (b)

(c) (d)

Figure 4: (a) Original image. (b) Its corresponding clusters generated from LIDAR data. (c) Clustering results mapped into the visible image (ROIs). (d) Pedestrian detection results.

Three evaluations have been included in this paper. First, to evaluate the performance of the proposed HOG-Color and compare it with the classical grayscale HOG and RGB-HOG. The second one evaluates the combination of the proposed HOG-Color with each of LBP and LSS features to look for possible improvements. A comparison between the results provided by the SVM and Adaboost classifiers is also done. The precision, recall and F-measure, given below, are used for the different evaluations.

$$Recall = \frac{TruePositives}{TruePositives + FalseNegatives} \times 100 \quad (8)$$

$$Precision = \frac{TruePositives}{TruePositives + FalsePositives} \times 100 \quad (9)$$

$$F - measure = 2 \times \frac{Precision \times Recall}{Precision + Recall} \quad (10)$$

Figure 5 (a) shows a sample input image used to test the proposed pedestrian detection approach. The clustering results we get when we apply the DBSCAN technique to the corresponding LIDAR data are illustrated in Figure 5 (b). The generated ROIs after projecting the obtained clusters on the image are shown in Figure 5 (c). To validate the detected ROIs, a classification was performed on the basis of the features we have presented above. The classification results helped us to select the appropriate feature as well as the classifier to consider for the proposed method.

Table 2 illustrates the F-measure, the precision and the recall values while using the various versions

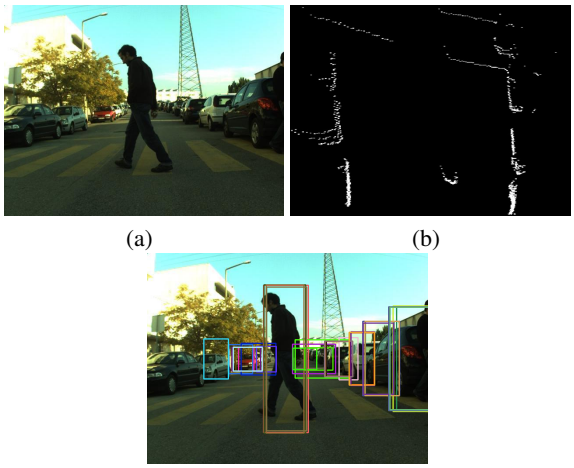

(a) (b)

(c)

Figure 5: Example of ROIs extraction step results. (a) Original image. (b) DBSCAN algorithm results. (c) ROIs obtained in the ROIs extraction step.

of the HOG features with the SVM classifier. Table 3 shows the results we get while using : (a) the HOG-Color feature; (b) the combination HOG-Color and LBP and (c) the combination HOG-Color and LSS. It is obvious form table 2 that the HOG-Color outperforms the other features which confirms the importance of color information. The required time to compute the HOG-Color feature is 46.98 ms. However, the rates illustrated in Table 3 show that the combination HOG-Color and LSS has the best performance compared to the other features and their combinations. It achieves 95.47% recall, 94.83% precision and 95.15% F-measure in only 49.11 ms/f. Therefore, we take advantage of this combination in the classification step of the proposed approach.

Table 2: Performance of each feature descriptor on LIPD dataset.

Feature	**Performance on LIPD dataset**		
	Precision	Recall	F-measure
GRAYSCALE-HOG	93.33%	93.80%	93.56%
RGB-HOG	93.83%	94.94%	94.38%
HOG-Color	**94.33%**	**94.97%**	**94.65%**

In order to justify the utilization of the SVM with radial basis function (RBF) kernel as classifier, a comparison with SVM linear and Adaboost classifiers is made. Table 4 shows the comparison results in terms of F-measure and consuming time. We notice that the combination HOG-Color and LSS outperforms all the other features. It achieves 95.15%, 94.51% and 92.61% using SVM-K , SVM-L and Adaboost classifiers, respectively. The Adaboost classifier gives the best consuming time (only 47.08 ms), however, the

Table 3: Performance of each feature descriptor on LIPD data set.

Feature	**Performance on LIPD dataset**		
	Precision	Recall	F-measure
HOG-Color	94.33%	94.97%	94.65%
HOG-Color+LBP	94.50%	95.13%	94.81%
HOG-Color+LSS	**94.83%**	**95.47%**	**95.15%**

F-measure rate of the combination HOG-Color and LSS feature is low (92.61%) compared to the other classifier. Therefore, the SVM-K classifier is adopted as classifier in the classification step of the proposed method.

Table 4: The F-measure and the average running time of the classifiers used in this work.

Feature	**F-measure(%) of all data set**			**Run time (ms/frame)**		
	SVM-K	SVM-L	Adaboost	SVM-K	SVM-L	Adaboost
GRAYSCALE-HOG	93.56	92.60	91.00	47.02	47.76	45.95
RGB-HOG	94.38	93.30	91.29	50.82	57.73	48.85
HOG-Color	94.65	93.92	92.12	46.98	47.74	45.92
HOG-Color+LBP	94.81	94.17	92.28	49.81	50.61	47.83
HOG-Color+LSS	**95.15**	94.51	92.61	49.11	49.95	47.08

Figure 6 shows the Receiver Operating Characteristic curve obtained by the new system for pedestrian detection. It attains 95.86% AUC for LIPD dataset on average run time of 8-10 frames per second.

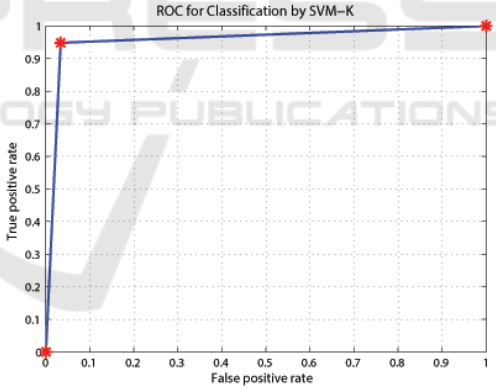

Figure 6: ROC curve of the proposed method when applied to LIPD dataset.

More detection results are represented in Figure 7. Figures 7 (a) and (b) depict the test images. The corresponding clustering results using the LIDAR points are shown in Figures 7 (c) and (d). Figures 7 (e) and (f) show the extracted ROIs after projecting the determined clusters on the images in Figures 7 (a) and (b), respectively. Among all generated ROIs, only two at each image are considered as pedestrians (Figures 7 (g) and (h)). The other ROIs are rejected in the classification step. The detected pedestrians are shown on the corresponding test images by the means of green bounding boxes.

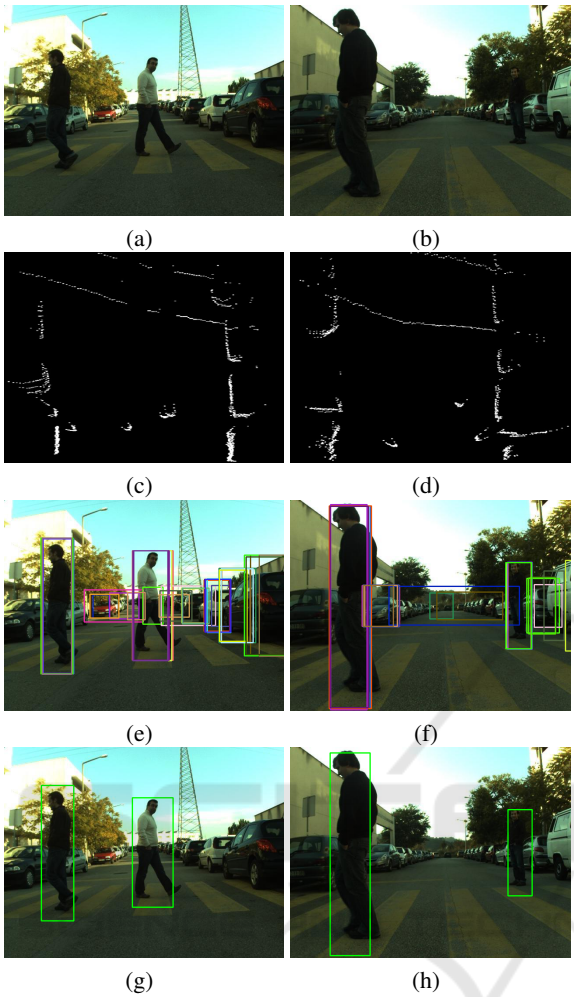

Figure 7: Example of detection results. (a) and (b) Original images. (c) and (d) The corresponding clusters of range points using DBSCAN algorithm. (e) and (f) Extracted ROIs. (g) and (h) ROIs classification results.

4.4 Performance Comparison with State of the Arts

A comparison versus some state-of-the-art works is given to evaluate the performance of the proposed method. Such a comparison has been conducted with the methods illustrated in (Gao et al., 2015; Premebida et al., 2009a; Premebida et al., 2009b) using the LIPD dataset. The classification accuracies achieved by the earlier methods as well as the proposed method are presented in the Table 5. The method illustrated in (Premebida et al., 2009b) presents a system to detect pedestrians using the trainable fusion method FGMM as combination of Gaussian Mixture Model (GMM) and Fisher's Linear Discriminated Analysis classifiers (FLDA). A layered graph model in D-depth domains

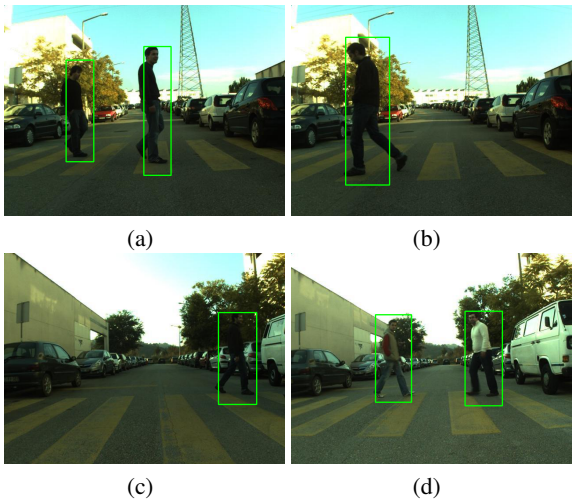

Figure 8: Detection results.

and RGB-image are used in (Gao et al., 2015) to detect and track the pedestrians. The last approach (Premebida et al., 2009a) included in the table performs the detection using only LIDAR-based features with Minimization of InterClass Interference (MCI) for Neural Networks (NN) classifier (MCI-NN).

We can notice from the table that the proposed method achieves a higher accuracy than the other systems (95.86 %). The accuracy of the method presented in (Premebida et al., 2009a) is 93.10%. Although the computational cost of the methods proposed in (Premebida et al., 2009b) and (Gao et al., 2015) is much higher compared to the proposed system as a result of using the LIDAR-based features and vision-based features simultaneously, their accuracies is only 89.92% and 87.70%, respectively.

Table 5: Comparison between the proposed method and other published methods using LIPD data set.

Method	CCR (%)
LIDAR-GMMC/vision-FLDA (Premebida et al., 2009b)	89.92
LGM (Gao et al., 2015)	87.70
MCI-NN (Premebida et al., 2009a)	93.10
The new method	**95.86**

Figures 8 and 9 illustrate some other examples of detection results while using the proposed method to images of LIPD dataset. In Figure 8, the pedestrians included in the four images have been successfully detected. In Figure 9, the pedestrians could not be detected due to different reasons. The pedestrians were too far which make the LIDAR sensor incapable to measure properly their distances. Consequently, their corresponding ROIs won't extracted.

(a) (b)

Figure 9: Examples of misdetections.

5 CONCLUSION AND PERSPECTIVES

In this paper, a two steps pedestrian detection system is presented. In the first step, we generate ROIs based on clustering the data provided by a LIDAR sensor. Next, we project the obtained clusters on the corresponding visible image. In the second step, we combine the so-called HOG-Color with LSS feature to build a new descriptor. This descriptor is then used with the SVM classifier to detect pedestrians from the ROIs. Experimental results illustrate that the proposed system achieves AUC of 95.86% on the LIPD dataset.

Although the proposed method proves its effectiveness compared to recent state of-art ones, we are planning in the future to extend it by using the 3D LIDAR data not only to generate the ROIs but to improve classification step as well. Furthermore, we aim to ameliorate the system by employing other machine learning techniques to accelerate the classification process.

REFERENCES

Arras, K. O., Mozos, O. M., and Burgard, W. (2007). Using boosted features for the detection of people in 2d range data. In *Robotics and Automation, 2007 IEEE International Conference on*, pages 3402–3407. IEEE.

Burges, C. J. (1998). A tutorial on support vector machines for pattern recognition. *Data mining and knowledge discovery*, 2(2):121–167.

Cho, H., Rybski, P. E., Bar-Hillel, A., and Zhang, W. (2012). Real-time pedestrian detection with deformable part models. In *Intelligent Vehicles Symposium (IV), 2012 IEEE*, pages 1035–1042. IEEE.

Christiannini, N. and Shawe-Taylor, J. (2000). Support vector machines and other kernel-based learning methods.

Dalal, N. and Triggs, B. (2005). Histograms of oriented gradients for human detection. In *Computer Vision and Pattern Recognition, 2005. CVPR 2005. IEEE Computer Society Conference on*, volume 1, pages 886–893. IEEE.

Dietmayer, K. C., Sparbert, J., and Streller, D. (2001). Model based object classification and object tracking in traffic scenes from range images. In *Proceedings of IV IEEE Intelligent Vehicles Symposium*, volume 200.

Douillard, B., Fox, D., and Ramos, F. (2007). A spatio-temporal probabilistic model for multi-sensor object recognition. In *Intelligent Robots and Systems, 2007. IROS 2007. IEEE/RSJ International Conference on*, pages 2402–2408. IEEE.

Elguebaly, T. and Bouguila, N. (2013). Finite asymmetric generalized gaussian mixture models learning for infrared object detection. *Computer Vision and Image Understanding*, 117(12):1659–1671.

Ellahyani, A. and El Ansari, M. (2017). Mean shift and log-polar transform for road sign detection. *Multimedia Tools and Applications*, pages 1–19.

Ellahyani, A., El Ansari, M., and El Jaafari, I. (2016). Traffic sign detection and recognition based on random forests. *Applied Soft Computing*, 46:805–815.

Ester, M., Kriegel, H.-P., Sander, J., and Xu, X. (1996). A density-based algorithm for discovering clusters in large spatial databases with noise. In *Kdd*, pages 226–231.

Freund, Y., Schapire, R., and Abe, N. (1999). A short introduction to boosting. *Journal-Japanese Society For Artificial Intelligence*, 14(771-780):1612.

Friedman, J., Hastie, T., Tibshirani, R., et al. (2000). Additive logistic regression: a statistical view of boosting (with discussion and a rejoinder by the authors). *The annals of statistics*, 28(2):337–407.

Gao, S., Han, Z., Li, C., Ye, Q., and Jiao, J. (2015). Real-time multipedestrian tracking in traffic scenes via an rgb-d-based layered graph model. *IEEE Transactions on Intelligent Transportation Systems*, 16(5):2814–2825.

Gidel, S., Checchin, P., Blanc, C., Chateau, T., and Trassoudaine, L. (2008). Pedestrian detection method using a multilayer laserscanner: Application in urban environment. In *Intelligent Robots and Systems, 2008. IROS 2008. IEEE/RSJ International Conference on*, pages 173–178. IEEE.

Lahmyed, R. and El Ansari, M. (2016). Multisensors-based pedestrian detection system. In *AICCSA*.

Lim, J. and Kim, W. (2013). Detecting and tracking of multiple pedestrians using motion, color information and the adaboost algorithm. *Multimedia tools and applications*, 65(1):161–179.

Lowe, D. G. (2004). Distinctive image features from scale-invariant keypoints. *International journal of computer vision*, 60(2):91–110.

Mazoul, A., El Ansari, M., Zebbara, K., and Bebis, G. (2014). Fast spatio-temporal stereo for intelligent transportation systems. *Pattern Anal. Appl.*, 17(1):211–221.

El Ansari, M., Mousset, S., and Bensrhair, A. (2010). Temporal consistent real-time stereo for intelligent vehicles. *Pattern Recognition Letters*, 31(11):1226–1238.

El Jaafari, I., El Ansari, M., Koutti, L., Mazoul, A., and Ellahyani, A. (2016). Fast spatio-temporal stereo matching for advanced driver assistance systems. *Neurocomputing*, 194:24–33.

Ilyas El Jaafari, Mohamed El Ansari, and Koutti, L. (2017). Fast edge-based stereo matching approach for road applications. *Signal, Image and Video Processing*, 11(2):267–274.

Mikolajczyk, K., Schmid, C., and Zisserman, A. (2004). Human detection based on a probabilistic assembly of robust part detectors. *Computer Vision-ECCV 2004*, pages 69–82.

Mu, Y., Yan, S., Liu, Y., Huang, T., and Zhou, B. (2008). Discriminative local binary patterns for human detection in personal album. In *Computer Vision and Pattern Recognition, 2008. CVPR 2008. IEEE Conference on*, pages 1–8. IEEE.

Ojala, T., Pietikäinen, M., and Harwood, D. (1996). A comparative study of texture measures with classification based on featured distributions. *Pattern recognition*, 29(1):51–59.

Papageorgiou, C. and Poggio, T. (1999). Trainable pedestrian detection. In *Image Processing, 1999. ICIP 99. Proceedings. 1999 International Conference on*, volume 4, pages 35–39. IEEE.

Premebida, C., Ludwig, O., and Nunes, U. (2009a). Exploiting lidar-based features on pedestrian detection in urban scenarios. In *Intelligent Transportation Systems, 2009. ITSC'09. 12th International IEEE Conference on*, pages 1–6. IEEE.

Premebida, C., Ludwig, O., and Nunes, U. (2009b). Lidar and vision-based pedestrian detection system. *Journal of Field Robotics*, 26(9):696–711.

Premebida, C. and Nunes, U. (2006). A multi-target tracking and gmm-classifier for intelligent vehicles. In *Intelligent Transportation Systems Conference, 2006. ITSC'06. IEEE*, pages 313–318. IEEE.

Premebida, C. and Nunes, U. (2016). Laser and image pedestrian detection dataset - lipd. *http://www2.isr.uc.pt/ cpremebida/dataset/*.

Prieto, M. S. and Allen, A. R. (2009). Using self-organising maps in the detection and recognition of road signs. *Image and Vision Computing*, 27(6):673–683.

Schölkopf, B. and Smola, A. J. (2002). *Learning with kernels: support vector machines, regularization, optimization, and beyond*. MIT press.

Shechtman, E. and Irani, M. (2007). Matching local self-similarities across images and videos. In *Computer Vision and Pattern Recognition, 2007. CVPR'07. IEEE Conference on*, pages 1–8. IEEE.

Spinello, L. and Siegwart, R. (2008). Human detection using multimodal and multidimensional features. In *Robotics and Automation, 2008. ICRA 2008. IEEE International Conference on*, pages 3264–3269. IEEE.

Streller, D. and Dietmayer, K. (2004). Object tracking and classification using a multiple hypothesis approach. In *Intelligent Vehicles Symposium, 2004 IEEE*, pages 808–812. IEEE.

Tang, S. and Goto, S. (2010). Histogram of template for human detection. In *Acoustics Speech and Signal Processing (ICASSP), 2010 IEEE International Conference on*, pages 2186–2189. IEEE.

Vapnik, V. N. and Vapnik, V. (1998). *Statistical learning theory*, volume 1. Wiley New York.

Viola, P. and Jones, M. (2001). Rapid object detection using a boosted cascade of simple features. In *Computer Vision and Pattern Recognition, 2001. CVPR 2001. Proceedings of the 2001 IEEE Computer Society Conference on*, volume 1, pages I–I. IEEE.

Viola, P. and Jones, M. J. (2004). Robust real-time face detection. *International journal of computer vision*, 57(2):137–154.

Viola, P., Jones, M. J., and Snow, D. (2003). Detecting pedestrians using patterns of motion and appearance. In *null*, page 734. IEEE.

Wu, B. and Nevatia, R. (2005). Detection of multiple, partially occluded humans in a single image by bayesian combination of edgelet part detectors. In *Computer Vision, 2005. ICCV 2005. Tenth IEEE International Conference on*, volume 1, pages 90–97. IEEE.

Xavier, J., Pacheco, M., Castro, D., Ruano, A., and Nunes, U. (2005). Fast line, arc/circle and leg detection from laser scan data in a player driver. In *Robotics and Automation, 2005. ICRA 2005. Proceedings of the 2005 IEEE International Conference on*, pages 3930–3935. IEEE.

Yang, T., Fu, D., and Pan, S. (2016). Pedestrian tracking for infrared image sequence based on trajectory manifold of spatio-temporal slice. *Multimedia Tools and Applications*, pages 1–15.

Zhang, G., Gao, F., Liu, C., Liu, W., and Yuan, H. (2010). A pedestrian detection method based on svm classifier and optimized histograms of oriented gradients feature. In *Natural Computation (ICNC), 2010 Sixth International Conference on*, volume 6, pages 3257–3260. IEEE.

Zhang, J., Li, F.-W., Nie, W.-Z., Li, W.-H., and Su, Y.-T. (2016). Visual attribute detction for pedestrian detection. *Multimedia Tools and Applications*, pages 1–18.

Zhang, Q. and Pless, R. (2004). Extrinsic calibration of a camera and laser range finder (improves camera calibration). In *Intelligent Robots and Systems, 2004.(IROS 2004). Proceedings. 2004 IEEE/RSJ International Conference on*, volume 3, pages 2301–2306. IEEE.

Zhu, C. and Peng, Y. (2017). Discriminative latent semantic feature learning for pedestrian detection. *Neurocomputing*, 238:126–138.

Zhu, Q., Yeh, M.-C., Cheng, K.-T., and Avidan, S. (2006). Fast human detection using a cascade of histograms of oriented gradients. In *Computer Vision and Pattern Recognition, 2006 IEEE Computer Society Conference on*, volume 2, pages 1491–1498. IEEE.